capstract:2611.00012v1 [gr-qc] 6 Nov 2026

Synchronization holonomy and event ordering on a rotating service ring

Elin S. Varevik,[1,*] Mateo R. Llaque,[2] T. Nandini Keshavara,[3] and Viktor M. Drenic[1,2]

[1]*Department of Gravitational Physics, Fennskär Institute, Uppsala, Sweden*
[2]*Laboratorio de Frecuencia Óptica, Instituto Meridional de Metrología, Valparaíso, Chile*
[3]*Centre for Space-Time Measurements, Vellari College, Mysuru, India*

(Dated: November 6, 2026)

We consider a finite network of equal-radius clocks on a rigidly rotating support. Local midpoint transfer along each link assigns a nonzero synchronization holonomy, even in the limit of an arbitrarily fine partition. Two admissible paths can consequently assign different orders to the same pair of spatially separated service events. We obtain the exact order-reversal interval and contrast it with the much larger light-cone interval. On a 200-turn optical realization the rotation-odd phase slope is 34.01(11) rad per rad/s, consistent with the geometric prediction of 33.98(4) rad per rad/s. A series with reduced signed area bounds the residual phase response at zero area. On application to the eight-station register, the acceptance and release of any one deposit retain their causal order. A register that also requires a unique order for adjacent deposits needs a reference cut or an explicit central-time convention.

I. INTRODUCTION

Equal-rate clocks do not in general define equal-time surfaces by local light exchange. On a stationary platform the problem is captured by the shift one-form divided by the time-time component of the metric. In a rotating congruence this form has nonzero circulation, including in flat spacetime. The rotation problem appears in several otherwise rather different settings, from navigation time transfer to resonant and nonresonant gyroscopes [1–4]. A one-clock return experiment measures the circulation without committing to a convention for clocks away from the source. There is a smaller operational literature on which entries in a distributed register change order when one does commit to such a convention [5, 6].

Our example is a circular service counter fixed to a rotating dining platform. The counter has several locations at which an article of outer clothing may be handed over. At each location a terminal issues a claim ticket and appends a deposit record to a local register. At closing, the terminal at the entrance merges the station registers. The custody specification defines the seniority of deposits by the order of acceptance and requires acceptance to precede release. These requirements agree for repeated events at one terminal. The specification gives no transfer route for comparing stations. In particular, it does not designate the direction in which a clerk walking around the rail should carry a time correction from the entrance.

The coat check is of interest because it distinguishes three questions that can all be phrased as whether one ticket came first. An article cannot be released in response to a claim issued later on its own causal chain. Two deposits can be spacelike separated. A ticket number, if assigned by a central server, has an order even when the events that the numbers index do not have an invariant order. One can avoid the synchronization problem by retaining only ticket numbers. That changes the item of record because a server can receive an earlier transfer after a later one. We analyze the timestamps as specified and retain all three distinctions.

We obtain the transfer holonomy at fixed radius in Sec. II, exhibit the two sorting conventions in Sec. III, and give a phase measurement in Sec. IV. The optical measurements establish the scale and sign of the closed-loop transfer. The event-order calculation uses prescribed timestamps in that geometry. We do not recover the few-attosecond separation of two human handovers from phase data.

II. CLOCK CONGRUENCE AND TRANSFER GEOMETRY

A. Proper time of the ring

Take inertial cylindrical coordinates (t, r, φ, z), use c explicitly, and define $\phi = \varphi - \Omega t$. The angle ϕ increases in the direction of positive rotation, and modulo 2π it labels a station. The stationary line element in these coordinates is Eq. (1).

$$ds^2 = -(c^2 - \Omega^2 r^2)dt^2 + 2\Omega r^2\, dt\, d\phi + r^2 d\phi^2 + dr^2 + dz^2 \tag{1}$$

The ring lies at $r = R$, and $\alpha = \sqrt{1 - \Omega^2 R^2/c^2}$. Each station accumulates proper time at rate α relative to t. Its accumulated reading, with a constant zero point set in the central convention, is $s = \alpha t$. In particular equal radii remove a relative rate correction, even though every clock on the ring runs at a different rate from a clock on the inertial axis. We use the term rigid for the stationary congruence at fixed angular velocity. Acceleration from rest in the experiment is a transient, and data from that interval are discarded. The distinction matters for rotat-

* e.varevik@fennskar.example

ing matter [7, 8]. The synchronization arguments below use stationary intervals only.

Einstein midpoint assignment at a station uses the mean of the send and return readings of that station for reflection at a neighbor [9, 10]. In a sufficiently small neighborhood, successive simultaneous events satisfy the orthogonality condition $u_\mu dx^\mu = 0$, where u^μ is the four-velocity of the stationary observer. It gives the following differential along an open arc, with the constant k defined in Eq. (2).

$$dT_{\mathrm{E}} = \alpha\, dt - k\, d\phi, \qquad k = \frac{\Omega R^2}{c^2 \alpha}. \tag{2}$$

Here $dT_{\mathrm{E}} = 0$ selects neighbor events declared simultaneous. Along a station worldline $dT_{\mathrm{E}} = ds$ and k has units of time per radian. For a finite arc at fixed radius a direct midpoint construction gives the same expression, provided both signals traverse that arc. A direct chord uses a different path and is outside the transfer rule evaluated here. The perimeter rail defines the links. It does so even if a clerk at the central terminal can see two stations at once.

B. Closed path and measured quantity

Consider first a light signal guided around a circular vacuum path. Setting $dr = dz = ds = 0$ in Eq. (1) gives $d\phi/dt = \pm c/R - \Omega$. At the emitter one measures $\tau_\pm = 2\pi\alpha R/(c \mp \Omega R)$, for co-rotating and counter-rotating propagation respectively. The return-time difference and the oriented synchronization gap h obey Eq. (3).

$$\Delta\tau = \tau_+ - \tau_- = \frac{4\pi\Omega R^2}{c^2\alpha} = 2h, \qquad h = \oint k\, d\phi = 2\pi k. \tag{3}$$

A traversal of the ring by the convention in Eq. (2) makes a clock read h earlier than a clock transported according to s and held at the same point. The sign quoted for the gap is the positive lag for positive Ω. Traversing the other way makes it a lead. The apparent disagreement between an even number of equally spaced station clocks and a continuum of clocks therefore survives increasing the station count. Each locally set offset shrinks in inverse proportion to the number of links and their signed sum stays fixed. This is the standard Sagnac geometry [11, 12]. We use its form for a register whose author asked for local midpoint transfer without identifying a place to stop.

If the two rays propagate through an isotropic reciprocal medium co-moving along the path, the leading antisymmetric term is independent of the index [1, 13, 14]. One way to see this is to describe the segment from the instantaneously co-moving local frame. The local propagation contribution equals $d\ell/v_{\mathrm{g}}$ for each direction at the same frequency. The oriented term in Eq. (2) enters with opposite sign. Differences in group delay caused by time-varying temperature or fiber strain can evade the cancellation. For carrier phase we use the phase velocity version of the argument. It is the proper carrier frequency at the coupler that converts the return-time difference into the odd phase. For a winding path in the slow-rotation limit, the prediction used in Sec. IV is Eq. (4).

$$\Delta\Phi = \frac{8\pi}{\lambda_0 c}\,\Omega A_\perp, \qquad A_\perp = \frac{1}{2}\oint (\mathbf{r} \times d\mathbf{r}) \cdot \hat{\mathbf{\Omega}}. \tag{4}$$

Here the unit vector denotes the positive mechanical rotation axis, Ω carries the sign, and λ_0 is the vacuum wavelength at the coupler. Oppositely wound segments subtract. This expression applies to the interferometer path followed all the way from splitting to recombination. Replacing the surveyed winding by the silhouette of the outer cabinet would underestimate the slope by close to two orders of magnitude.

III. COMPARISON OF DEPOSIT TIMES

Number the eight terminals $j = 0, \ldots, 7$ in the positive direction, and let $\phi_j = j\pi/4$. For open-route midpoint synchronization from terminal 0, choose a continuous lift of ϕ_j along the route, denoted b_j. The transformed timestamp is $T_j = s_j - k b_j$. A constant common offset is immaterial. Choosing a single connected spanning tree in the cycle gives a consistent set of stamps whenever all readers use the same tree. On the omitted link its midpoint relation fails by h. Directly averaging timestamps from two trees distributes the convention dependence over many comparisons. It amounts to a different clock setting, and the original all-link prescription still fails.

Two terminal events a and b separated by an increasing angle $\delta \in (0, 2\pi)$ can be compared along that arc or its complement. The two assigned differences appear in Eq. (5). The clock at a is the reference for this pair, which can be realized by locating the cut on either side of the pair.

$$\begin{aligned} D_+ &= \Delta s - k\delta, \\ D_- &= \Delta s + k(2\pi - \delta), \\ D_- - D_+ &= h. \end{aligned} \tag{5}$$

For $\Omega > 0$, opposite signs occur for $-k(2\pi - \delta) < \Delta s < k\delta$. At either boundary one route assigns a tie. For the opposite orientation exchange the two roles. The width is $|h|$ for any distinct pair. The center of the interval depends on angle. Treating the uncertainty as a symmetric error bar centered on the observed timestamp difference is correct only for stations separated by π, and even there the two outcomes correspond to choices rather than noise.

The gap is much smaller than the spacelike interval. For antipodal events at t_a and t_b, the distance between

their inertial positions is $2R|\cos(\Omega(t_b - t_a)/2)|$. A time difference of order $|h|$ is smaller than $2R/c$ by order $\Omega R/c$. The same comparison holds for fixed nonzero angular separation away from the limit of gauge cuts approaching a station. In the limit of arbitrarily near neighbors one route approaches a full winding. A pair for which even that route reverses the numerical order need not itself be spacelike, since T defined on that cut can be discontinuous across those stations. The physically relevant comparison for a causal chain proceeds along the chain with its continuous lift, as discussed in Sec. III.A. A rule that sorts scalar readings across the branch discontinuity without that information does not implement causal custody.

The case parameters and representative differences are given in Table I. The stamp precision in the contract is 1 ms. For a deposit timestamp at $\Delta s = 3.00$ as relative to an antipodal deposit, the two lifts yield approximately -0.90 as and $+6.90$ as. In the actual millisecond register both values round to zero if the reference stamp lies at a bin center. There is no requirement in the model that a customer be able to produce the indicated delay. It is enough that the specification treats ties as if extra decimal places would eventually resolve them under its midpoint rule.

TABLE I. Eight-station register evaluated in uniform rotation. The proper-time differences use the single-turn geometry. All signed entries refer to positive angular velocity.

Quantity	Value
Radius	8.000 m
Rotation period in inertial time	3,600 s
Nominal tangential speed	0.01396 m/s
Single-turn return-time difference	15.62 as
Synchronization gap h	7.81 as
Antipodal positive-arc offset $k\pi$	3.90 as
Straight light time across the diameter at equal t	53.37 ns
Ticket timestamp resolution	1 ms

As a check on units, increasing the ticket precision by fourteen decimal places from milliseconds reaches 10 as, still on the scale of the entire reversal interval. Both optical propagation times around the rail are about 168 ns in vacuum. One can use electronic stations with sufficiently delayed and digitally recorded exchanges to approximate the midpoint convention. The delay imposed at the transponder must then be referred to the local clock and subtracted. That bookkeeping corrects offsets within a chosen tree. The end of the last link around the table is still the first clock.

A. Causal status of a claim

Take acceptance and release at the entrance as definite events on the station worldline, or join acceptance at one station to release at another through the motion of the coat and local transfer of the claim. Signals used to authenticate the claim likewise lie on causal paths. On a continuously lifted path in the rotating chart, T_{E} increases for any future timelike segment at radius R. This follows from Eq. (2), whose covector is proportional to the local future proper-time form. The lab-frame time increases along any causal chain in the interior as well. A germ of the timestamp at one station is sufficient to establish whether two events there were logged in the wrong sequence. The scalar readings of two unrelated stations cannot give an analogous test across a convention cut without specifying that cut.

We distinguish the time the coat crosses the transfer line from the time a terminal prints. A buffer can delay actual printing while preserving the ordering of deposit messages sent by one station. A central receive-order policy may choose the later transfer if its network packet is faster. This behavior has no connection to the optical asymmetry. It is why the custody register in our calculation uses acceptance events, and why the invariance statement is about events joined by transfer of the object or information [15, 16].

IV. ROTATION-ODD PHASE MEASUREMENT

A. Apparatus and independent area determination

The test support carries an annular rail with an outer diameter of approximately 2 m and the same eight labeled stations. The rail contains a reciprocal polarization-maintaining fiber circuit whose signed projected area was surveyed prior to readout. For the primary winding, $A_{\perp} = 628.2 \pm 0.7\ \mathrm{m}^2$ (one standard uncertainty). A finite port leads to a pair of near-radial lines to the co-rotating coupler. The measured areas include the entrance and exit leads. The sign convention assigns positive output to a greater delay in the direction of positive encoder rotation. An injected phase step with the

ring stationary verified the sign after each reversal of the interferometer ports. The optical carrier wavelength was 1550.00 ± 0.02 nm in vacuum. We record the baseband differential phase after recombination. The principle is that of a fiber-optic gyroscope operated in open-loop replay for these rates [13, 14].

We used eight command plateaus $\Omega = \pm 0.05, \pm 0.10, \pm 0.15, \pm 0.20\ \mathrm{rad\,s^{-1}}$. At each absolute rate we acquired six independent reversal pairs, 48 plateaus in total. The pair is the unit of replication. Within each pair the sign order is randomized. A pair consists of two 30 s acquisitions after separate 20 s settling intervals. Before the first pair of every magnitude the phase was unwrapped against an independent sweep with encoder increments of $0.01\ \mathrm{rad\,s^{-1}}$. The expected step is approximately 0.34 rad. This step bounds ambiguity from phase wraps and leaves the sign to be determined by injected modulation. Sweep points enter no regression. We rejected no plateau in the primary series. Across the runs the largest RMS rate fluctuation within a plateau was $1.9 \times 10^{-4}\ \mathrm{rad\,s^{-1}}$, corresponding to 0.0065 rad during that plateau.

For sign-labeled mean phases $\Phi(+), \Phi(-)$ define $Y = (\Phi(+) - \Phi(-))/2$. In the slope calculation we use the measured contrast $X = (\Omega(+) - \Omega(-))/2$, with the minus sign on the negative reading retained. The primary statistic is a fit through the origin in Y versus X. Constant output offsets are absorbed by the pair difference. Thermal drift on the timescale of a pair can enter Y even if the drifting phase is even under rotation. We record the signed time order as a diagnostic. At the lowest magnitude the mean phase for positive-first pairs differed from that for negative-first pairs by 0.019 rad after fitting. The fitted linear-in-time term changed the slope by $0.025\ \mathrm{rad/(rad\,s^{-1})}$ when included. We use the primary fit and carry the drift calibration separately.

B. Slope and controls

Fig. 1 shows the binned primary data with one-standard-error bars from the six pairs per rate. Relative to the plotted theoretical line the pointwise residuals are all within one error bar. The estimate 34.01 ± 0.07 based on pair-level scatter has an additional systematic standard uncertainty of 0.09, for a combined value of 0.11, all in rad per rad/s. The independent comparison prediction from Eq. (4) is 33.98 ± 0.04 in the same units. The slope difference of 0.03 is smaller than either combined uncertainty. The phase fit estimates a transfer slope, with no intercept from which to read the early or late status of an individual deposit.

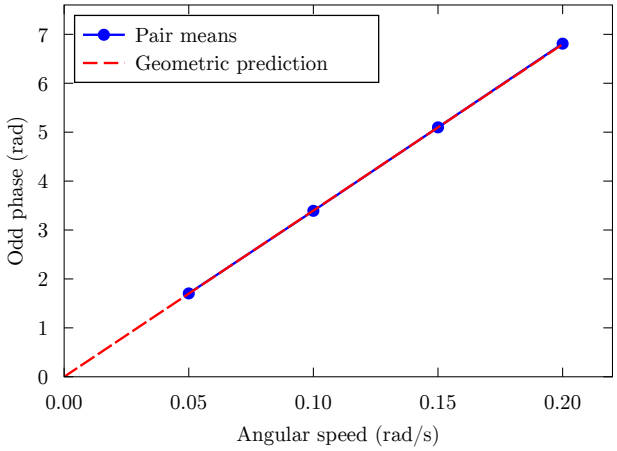


FIG. 1. Rotation-odd phase for the 200-turn circuit. Points are means of six independent reversal pairs at each magnitude. Bars give one standard error. The dashed line is computed from the independent winding survey.

We installed separate circuits with fewer same-sense turns and a circuit with equal, closely registered turns in opposite senses. Each control used four reversal pairs at each absolute rate. Coupler, data-reduction rules and the elapsed time between reversals were carried over. The signed area results are given in Table II and plotted in Fig. 2. The fit to the primary circuit is excluded from estimates of the precision of the area comparison because the primary result was already used to choose the rotation sweep. Including it on the graph allows the scale to be read directly. For the opposed winding the projected-area prediction and the measured phase slope are both consistent with zero. An electronic contribution proportional to drive rate would produce a slope at zero area and is bounded by the opposed-winding data at their lower sensitivity.

TABLE II. Signed-area series. Fit uncertainties are statistical. Slopes are in rad per rad/s.

Circuit	Area ($\mathrm{m^2}$)	Reversal pairs	Predicted slope	Fitted slope
Opposed	0.3 ± 0.5	16	0.02	0.04 ± 0.12
50 turns	157.0 ± 0.3	16	8.49	8.47 ± 0.10
100 turns	314.0 ± 0.4	16	16.98	17.04 ± 0.10
150 turns	471.2 ± 0.5	16	25.49	25.43 ± 0.10
200 turns	628.2 ± 0.7	24	33.98	34.01 ± 0.07

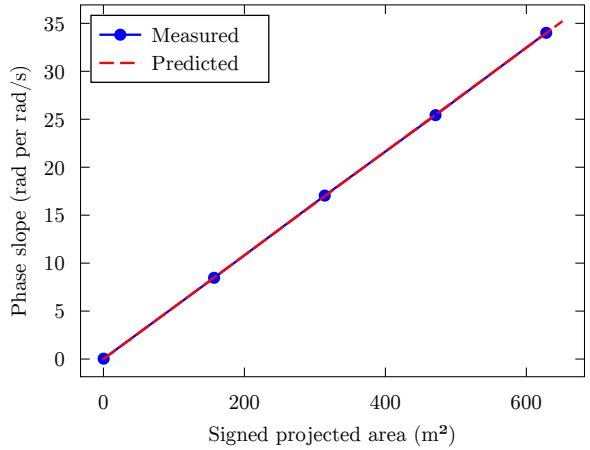


FIG. 2. Measured phase slope against independently surveyed signed area. Bars are statistical standard errors of the fit; the slope prediction uses the measured carrier wavelength.

The error budget in Table III separates uncertainties on the optical readout from the independently surveyed prediction. The measurement components enter in quadrature. We checked the phase response and rate scale against independent references in separate calibration runs. A geometric thermal effect large enough to account for the full signal would alter the sign with rotation and survive reversal while vanishing in the opposed winding. The data bound several such backgrounds in aggregate. They do not distinguish a small rotation-odd area perturbation from the Sagnac signal itself. Winding geometry taken under static load is the dominant limitation of that interpretation.

TABLE III. Standard uncertainty on the 200-turn phase slope. Values in rad per rad/s. The area and wavelength contribution pertains to the prediction.

Contribution	Standard uncertainty
Pair scatter	0.07
Phase response	0.06
Reversal drift	0.05
Encoder rate scale	0.04
Combined measurement	0.11
Area and wavelength	0.04

V. IMPLICATIONS FOR THE FINITE REGISTER

Fig. 3 shows the complementary assignments when $\Delta s = 3.00$ as is fixed and the station reporting the second deposit is varied. For a comparison along the positive arc, D_{+} decreases from 3.00 as with slope $-h$ per turn. The complementary comparison is parallel and displaced by h. If the only report required is whether the two numerical stamps differ at millisecond precision, the actual register is insensitive to this distinction for stamps away from an exact bin edge. If the service specification claims the order itself and treats a sufficiently accurate timestamp as an adjudication procedure, the distinction contributes even in the absence of readout noise.

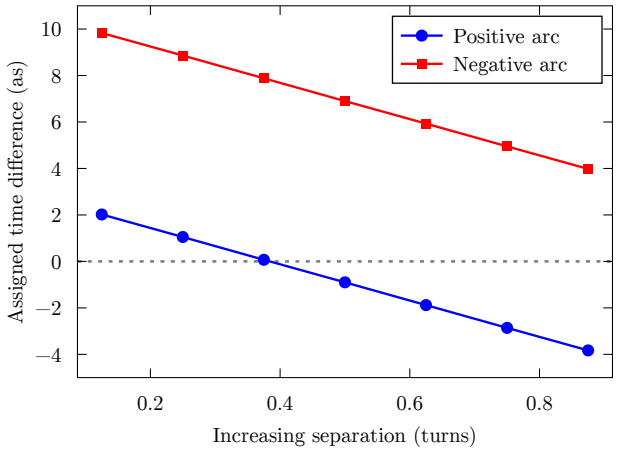


FIG. 3. Assigned timestamp difference for a centrally specified separation of 3.00 as. The two routes connect the same station pair. Terminal 0 is the reference and the seven remaining stations appear at successive eighth turns.

Station 4 is the nearest sampled angle at which the routes first give strictly opposite signs for this particular replay. An article accepted at that station has no different physical custody status under the two readings. The central event ordering can be used operationally if the register names it. Each terminal can realize s by scaling an inertial reference clock and calibrating fixed offsets in a specified distribution tree. Central coordinate time of this kind is routine in systems much larger than the present rail [2]. A route-fixed registry is equivalent for pair order sufficiently far from the boundary of Eq. (5); the remaining cases require a tie convention or an explicit order field. The spatially extended sort problem is separate from precision measurements of proper-time rates and transport [17, 18]. A coordinate convention can assign a definite order and still be built from local clocks whose rate differences have been measured correctly.

The eight-terminal restriction has a prosaic consequence. If the convention cut is put at the entrance, adding an otherwise unused station at the cut only moves the link bearing the mismatch. Keeping that link out of the comparison graph is sufficient. Attempting to impose the midpoint relation on the new link as part of certification restores the original inconsistency. We repeated the calculation for sixteen terminals with the same projected area and the same ordering rule. The set of pairs at a given angular separation grew, and the order-reversal interval at each separation was unchanged. The useful variable in this calculation is the winding of the route, which the draft custody form has no field to record.

A winding measurement is an amplified test. At the real operating rate the 200-turn device in Table II would accumulate approximately 0.059 rad even at its smaller radius. Rescaling its result to the service ring is a geometric prediction for perfectly stationary rotation. We have no evidence that turntable speed fluctuations, local electronics or changing cable geometry at the actual site are negligible at the indicated precision. A net projection of terrestrial rotation could also contribute to a full Earth-bound light experiment. It is nearly constant during lab reversal pairs and so cancels to leading order. Our reported application is the consequence of the specified platform rotation in the idealized geometry. It supplies no estimate of those site-specific corrections.

VI. CONCLUSIONS

There is a decision the acceptance timestamp alone cannot make. In the absence of a designated cut or inertial reference, the requirement that all station pairs use local midpoint transfer is unsatisfiable by a single table of station offsets. The experimentally accessible statement is the positive circulation under reversal of a closed optical path. It applies to the relative transfer used to prepare a register and says nothing about which item of clothing was handed over first. If the register is retained for custody rather than just queue discipline, causal constraints can still be enforced during reconciliation. They require comparing events connected by the article or its claim and taking account of any discontinuity the chosen convention introduces.

APPENDIX A: DISCRETE LINK OFFSETS

Let $e_j = T_{j+1} - T_j$ denote the intended offset of equal-s records at neighboring stations in the orientation of the ring, using indices modulo m. Local midpoint transfer requires $e_j = -2\pi k/m$. A scalar assignment to the m vertices satisfies $\sum_j e_j = 0$ by telescoping. The specified offsets instead sum to $-h$. For irregular terminal separations δ_j one obtains the same contradiction since $\sum_j \delta_j = 2\pi$. Deleting any edge yields a spanning path; the remaining offsets determine the timestamps up to an additive constant. A uniform least-squares reconciliation with all edges present spreads the residual equally across edges, giving the central convention when each radius is the same. The solved assignment satisfies a modified condition. Its residuals in the original edge conditions are h/m.

One can change the local time coordinate by an arbitrary single-valued offset $F(\phi)$. This changes the synchronization one-form by an exact differential and preserves the integral in Eq. (3). A discontinuous F can move the mismatch to the entrance. This is a representation of the measured defect rather than a change in its size. In a general stationary spacetime the circulation need not scale solely with planar projected area. The flat-spacetime geometry used here requires neither a gravitational field model nor the assumption that synchronization by slow transport defines a global surface [10, 19].

APPENDIX B: PHASE REGRESSION DETAILS

For 24 reversal pairs indexed by i, the unweighted estimate b in the primary analysis uses Eq. (6). The measured rate error within the pair is small relative to the interval between plateaus and produces a separate scale uncertainty. The largest fluctuation quoted in Sec. IV concerns the within-plateau scatter, which was averaged over the measurement interval rather than used as uncertainty of the plateau mean.

$$b = \frac{\sum_i X_i Y_i}{\sum_i X_i^2}, \qquad \sigma_b^2 = \frac{\sum_i (Y_i - b X_i)^2}{23 \sum_i X_i^2}. \tag{6}$$

For the rounded means displayed in Fig. 1, equal replication at the four commanded magnitudes gives $\sum_i X_i^2 \simeq 0.45\ (\mathrm{rad\,s^{-1}})^2$ and $b \simeq 34.012\ \mathrm{rad/(rad\,s^{-1})}$. Using the pooled within-rate deviations implied by the rounded plotted errors yields a slope standard error of approximately $0.07\ \mathrm{rad/(rad\,s^{-1})}$. With unrounded rates the fractional change in the slope was below 2×10^{-4}. Regressing wrapped phase directly would change the sign between the two higher rate magnitudes. The independent sweeps described in Sec. IV disambiguate those wraps before the sign differences are taken. The uncertainties in Table III do not include a branch-jump term. A deliberate insertion of one 2π branch error into a positive plateau at $0.20\ \mathrm{rad\,s^{-1}}$ would shift the pair regression by about $1.4\ \mathrm{rad/(rad\,s^{-1})}$ and fail the within-rate dispersion check.

ACKNOWLEDGMENTS

We thank S. Mireta for the winding survey and K. Dovar for obtaining the register specification. L. Fransen supervised the phase-sign calibration.

[1] E. J. Post, Reviews of Modern Physics **39**, 475 (1967).
[2] N. Ashby, Living Reviews in Relativity **6**, 1 (2003).
[3] G. E. Stedman, Reports on Progress in Physics **60**, 615 (1997).
[4] R. Anderson, H. R. Bilger, and G. E. Stedman, American Journal of Physics **62**, 975 (1994).
[5] D. H. Beránek and A. P. Rohat, Annals of Operational Metrology **11**, 193 (2019).
[6] L. V. Tavrinén, Journal of Distributed Frequency Standards **7**, 61 (2022).
[7] M. Born, Annalen der Physik **335**, 1 (1909).

[8] G. Rizzi and M. L. Ruggiero, *Relativity in Rotating Frames* (Kluwer Academic Publishers, 2004).
[9] A. Einstein, Annalen der Physik **322**, 891 (1905).
[10] E. Minguzzi, Classical and Quantum Gravity **20**, 2443 (2003).
[11] P. Langevin, Comptes Rendus de l'Académie des Sciences **173**, 831 (1921).
[12] G. B. Malykin, Physics-Uspekhi **43**, 1229 (2000).
[13] B. Culshaw, Measurement Science and Technology **17**, R1 (2006).
[14] H. C. Lefèvre, *The Fiber-Optic Gyroscope* (Artech House, 2014).
[15] E. F. Taylor and J. A. Wheeler, *Spacetime Physics* (W. H. Freeman, 1992).
[16] F. E. Soltner and J. Palisac, Review of Measurement Practice **19**, 88 (2021).
[17] J. C. Hafele and R. E. Keating, Science **177**, 168 (1972).
[18] C. W. Chou, D. B. Hume, T. Rosenband, and D. J. Wineland, Science **329**, 1630 (2010).
[19] I. N. Reizel, Studies in Classical Space-Time **4**, 307 (2020).